

3D KINEMATICAL ANALYSIS OF LARGE SCALE SUBSTRATE SURFACE GRINDING

Libo ZHOU, Jun SHIMIZU, Kazuhiro SHINOHARA, Hiroshi EDA
Ibaraki University, Nakanarusawa 4-12-1, Hitachi-shi, JAPAN 316-8511

1. Introduction

In the previous report [1], an advanced grinding machine with the capability of one-stop finishing for $\phi 300\text{mm}$ Si wafer has been developed. The core technology is the GMM actuated positioning/alignment device which is able to position half a ton of payload at the resolution of 5 \AA and align tilt angle of α, β at the resolution of 0.1° . Use of state-of-the-art technologies developed for the grinding system have made it possible to precisely control the motion of each cutting edge, for example, to achieve the ductile mode machining. The behavior of each grain and its effect on surface generation become mathematically analytical in 2D or 3D manner. Taking one step further, this paper has developed a 3D model for infeed grinding which is often used in grinding systems for silicon wafer and other large scale substrates, and mathematically described the cutting path and its density. Being associated with the achievable surface roughness and global flatness, the simulation results are discussed and compared with the experimental results.

2. Infeed grinding Model

Most wafer grinding system utilizes the plunge (infeed) method [2] to keep the contact area unchanged and thereby to deliver a stable grinding performance throughout the grinding process. **Fig.1** shows a typical arrangement of the wheel and the wafer, where the wheel is half overlapped with the wafer. The grinding wheel is often shaped in a segmented ring with several millimeter thicknesses. When the wheel axis is aligned to be parallel to the wafer axis, the interaction between the wheel and wafer is made in X-Y plane. The two dimensional grinding model is schematically shown in **Fig.2**, where the relevant parameters are labeled. Corresponding to the alignment, in the 3D model, the tilts of wafer axis are defined as α and β respectively around X-axis and Y-axis. The other parameters used for analysis are listed in **Table 1**.

In a coordinate system that the origin is fixed at the center of the wafer, the three position components $[x(t), y(t), z(t)]$ of a grain, which is initially located at (r_1, θ_1) on the wheel, is specified as;

$$\begin{bmatrix} x(t) \\ y(t) \\ z(t) \end{bmatrix} = A \cdot B \cdot C \cdot D \begin{bmatrix} r_1 \\ L \\ -f \cdot t \end{bmatrix} \quad (1)$$

where the matrix A , D respectively represent the rotations of wafer and wheel, and are given as;

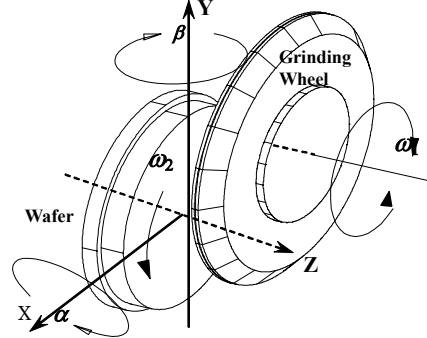


Fig.1 Grinding wheel/wafer arrangement

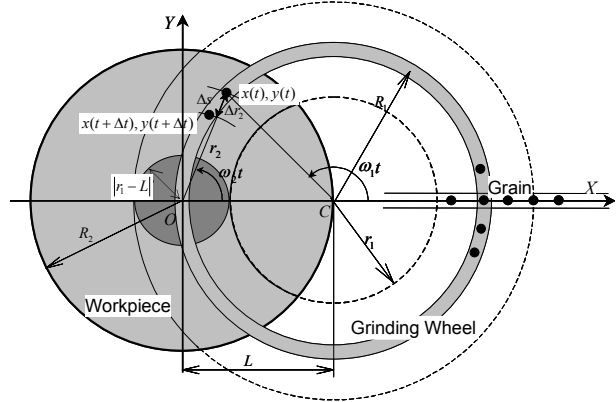


Fig.2 Grinding model

Table 1 Parameter list

| | |
|-------------------|---|
| R_1 | Wheel radius, 150mm or indicated otherwise |
| R_2 | Wafer radius, 150mm or indicated otherwise |
| (r_1, θ_1) | Grain initial position ($0 \leq r_1 \leq R_1, 0 \leq \theta_1 \leq 2\pi$) |
| r_2 | Position of machining point ($0 \leq r_2 \leq R_2$) |
| L | Offset between wheel axis and wafer axis |
| n_1 | Wheel rotational speed (+: CCW, -: CW) |
| n_2 | Wafer rotational speed (+: CCW, -: CW) |
| ω_1 | Wheel angular speed ($= 2\pi \cdot n_1$) |
| ω_2 | Wafer angular speed ($= 2\pi \cdot n_2$) |
| f | Infeed rate |
| t | Grinding time |
| Z_s | Infeed ($Z_s = f \cdot t$) |
| α | Wheel axis tilt around X-axis |
| β | Wheel axis tilt around Y-axis |

$$A = \begin{bmatrix} \cos \omega_2 t & \sin \omega_2 t & 0 \\ -\sin \omega_2 t & \cos \omega_2 t & 0 \\ 0 & 0 & 1 \end{bmatrix}$$

$$D = \begin{bmatrix} \cos \omega_1 t & 1 & 0 \\ \sin \omega_1 t & 0 & 0 \\ 0 & 0 & 1 \end{bmatrix}$$

while matrix B , C respectively express the tilts of wheel around X-axis and Y-axis, and are given as;

$$B = \begin{bmatrix} 1 & 0 & 0 \\ 0 & \cos \alpha & -\sin \alpha \\ 0 & \sin \alpha & \cos \alpha \end{bmatrix}$$

$$C = \begin{bmatrix} \cos \beta & 0 & \sin \beta \\ 0 & 1 & 0 \\ -\sin \beta & 0 & \cos \beta \end{bmatrix}$$

L is the offset between axes of the wafer and wheel and f represents the infeed rate. A grain which is initially located at (150, 0) is chosen for the case study of $\phi 300\text{mm}$ Si wafer. Shown in **Fig.3** is its cutting path made at different speed ratio n_2/n_1 and projected in X-Y plane. When $n_2/n_1 = 0.5$ the cutting path formed is a straight line. Other than that, lines are curved. It is important to note that the $n_2/n_1 = 1/3$ and $n_2/n_1 = 500/1500$ share the same pattern regardless of difference in each rotational speed. It is meant that the cutting path pattern is only determined by the speed ratio n_2/n_1 of the wafer against the wheel, not the individual revolution speed.

Since the matrix A , D are the periodic functions with respective period of $2\pi/\omega_2$ and $2\pi/\omega_1$. The least common period is then given as $2\pi \cdot k \cdot m \cdot n$. k, m, n should fulfill the following equation.

$$\frac{n_2}{n_1} = \frac{\omega_2}{\omega_1} = \frac{k \cdot n}{k \cdot m} \quad (k, m, n: \text{natural number}) \quad (2)$$

where k is the greatest divisor of ω_1 and ω_2 , while n/m is their irreducible fraction. It means within the first common period that one grain cuts the wafer once every rotation. From the second period onwards, the grain repeatedly goes through the same path so that the number of the cutting path formed is no longer increased. This is defined as the stable state. Comparing the stable states respectively made by $n_2/n_1 = 50/1500$ (or $1/30$) and $n_2/n_1 = 40/1500$ (or $2/75$), it is able to conclude that the number of the cutting path is determined by the denominator m .

3. Cutting path density and surface roughness

By examining the cutting path pattern shown in Fig.3, it

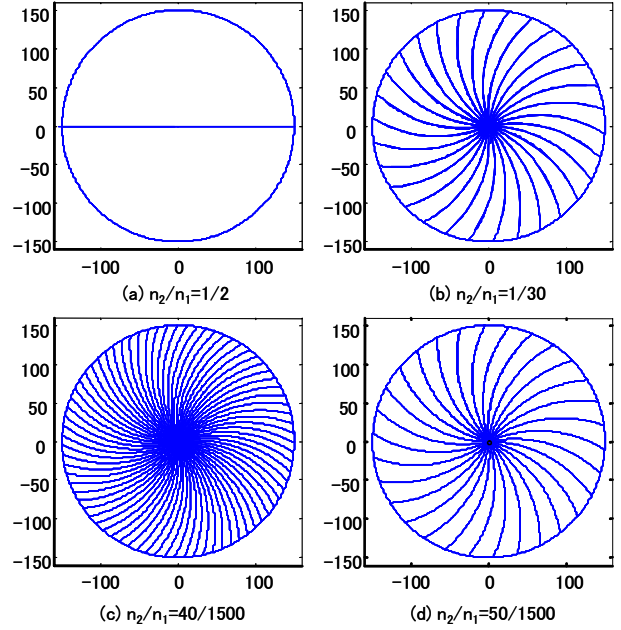


Fig. 3 Cutting path pattern

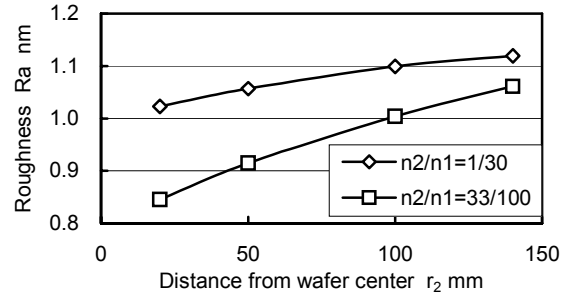


Fig. 4 Effect of cutting path density on Ra

is easily understood that the density of cutting path is higher in the wafer center than that at its fringe, and increases by increasing the denominator m . From the viewpoint of surface roughness, a large denominator m is preferable. **Fig.4** compares the surface roughness obtained from the different rotational speed combination. The cutting path at $n_2/n_1 = 495/1500$ (or $33/100$) is about three times denser than that at $n_2/n_1 = 50/1500$ (or $1/30$). It is clearly proven that the density of cutting path contributes to improvement in the surface roughness. In the meantime, an excessive m takes a long time to reach the stable state, which often leads to severe burn marks on the wafer surface. The result in Fig.4 also addresses a fact that the roughness obtained is inconsistent over the wafer surface, corresponding to the change in the density of cutting path.

Therefore, it is important to know the variation of the cutting path density at different radius r_2 . Form t

to $t + \Delta t$, the grain changes its position from $x(t), y(t)$ to $x(t + \Delta t), y(t + \Delta t)$ in X-Y plane. The increments in position are as;

$$\begin{cases} \Delta x = x(t + \Delta t) - x(t) \\ \Delta y = y(t + \Delta t) - y(t) \end{cases} \quad (3)$$

if the Δt is small enough, then the length of the cutting path formed in such short period is given as;

$$\Delta s \approx \sqrt{\Delta x^2 + \Delta y^2} \quad (4)$$

The change in the radius of the wafer is expressed as;

$$\Delta r_2 = \sqrt{x^2(t + \Delta t) + y^2(t + \Delta t)} - \sqrt{x^2(t) + y^2(t)} \quad (5)$$

Therefore, the cutting path density $d(r_2)$ at a specific wafer area is stated as;

$$d(r_2) = \lim_{t \rightarrow 0} \frac{m \cdot \Delta s}{2\pi r_2 \cdot \Delta r_2} = \frac{m}{2\pi} \cdot \frac{ds}{r_2 dr_2} \quad (6)$$

Fig.5 is the results calculated at different speed ratio, showing the density $ds/r_2 dr_2$ and the length change rate ds/dr_2 of the cutting path. No matter how the speed ratio changes, the cutting path density sharply increases toward to the wafer center and becomes infinite as radius r_2 takes zero. Mathematically, the center is a singular point for cutting path density. With such condition, the interference between wafer and wheel becomes irregular and creates an undesirable surface.

4. Cutting path density and flatness

The inconsistency of the cutting path density affects not only affects the surface roughness, but also the global flatness. As long as the loop stiffness of the machine tool is not infinite, higher cutting path density always leads to a higher removal of the material and results in a concave profile.

The 3D profile, which is obtained at grinding with a #3000 diamond wheel of 3mm thick segment, is shown in **Fig.6**. It is found that the profile at the wafer center is concaved as deep as $0.5\mu\text{m}$. The diameter of the hollow is approximately 3mm, exactly agrees with the wheel thickness. This problem remains unsolved as long as the wheel takes a ring shape.

More precisely, a ring type wheel can be considered as cutting edges uniformly distributing between external and internal radii. Therefore, its cutting path density is given in Eq.(7) by integrating the cutting path made by every grain which is located inbetween.

$$D(r_2) = \frac{m}{2\pi} \cdot \int_{r_i}^{r_1} \frac{ds}{r_2 dr_2} dr_1 \quad (7)$$

Fig.7 shows the density variation calculated on basis of the actual wheel dimension of $148.5 < r_1 < 151.5$. It is found that the density exactly takes a reverse form of Fig.6. This fact indicates that the material removal depth $h(r_2)$ is proportional to the cutting path density.

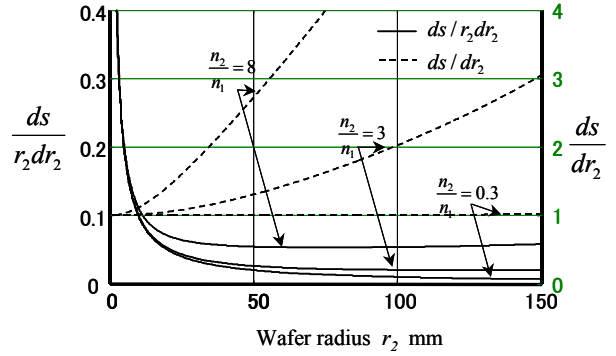


Fig. 5 Cutting path density and length ratio

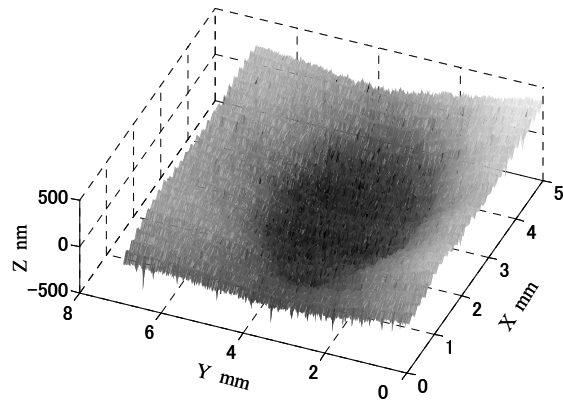


Fig. 6 Concave profile in wafer center

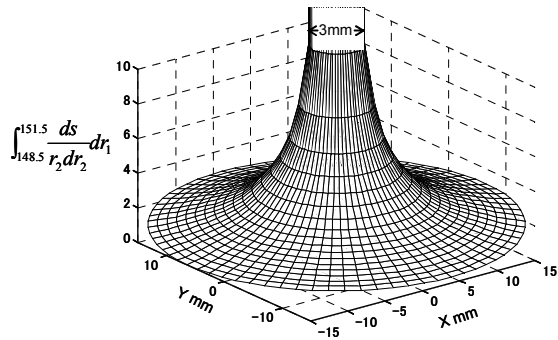


Fig. 7 3D cutting path density

A practical solution for solving the flatness problem is to tilt the axis of the wafer (or wheel) slightly inclining against the axis of the wafer [3], to offset the effect of unevenness of cutting path density. **Fig.8** is the cutting path, re-calculated at $\alpha = \pm 0.1^\circ$ and presented in 2D/3D graphs according to the Eq.(1). When the tilt is made around X-axis only, the profile takes a circular cone shape regardless of the direction of tilt. 0.1° in α creates a variation of profile in Z direction of about 0.2mm over 300mm. **Fig.9** shows the results when the wheel axis inclines around Y-axis. A positive β makes the profile convex, while a

negative β makes the profile concave. The effect of β on the global flatness is about half that of α .

From the results shown in Fig.6 ~ Fig.9, it is easy to understand that choosing an appropriate alignment α, β is able to counterbalance the profile error created by unevenness in the cutting path density. Taking in account of the geometrical form $z(r_2)$ made by alignment, when the removal depth $h(r_2)$ meet the following condition, a flat surface is achievable.

$$h(r_2) = z(r_2) - \lambda \cdot D(r_2) = \text{constant} \quad (8)$$

where λ is a constant associating the removal depth with the cutting path density. As described in the previous report, the grinding machine developed in this project is equipped with a GMM alignment plate, able to tilt 0.1 second over the range of ± 1.5 degrees around both X- and Y-axis. For this particular case of $\phi 300\text{mm}$ Si wafer, the wafer axis is aligned at $\alpha = 0.001^\circ$ and $\beta = -0.001^\circ$. After grinding, as shown in Fig.10, the global flatness is significantly improved up to $0.2\mu\text{m}/300\text{mm}$. This result demonstrates how important the alignment mechanism is for infeed grinding to improve the global flatness.

5. Conclusion

In this report, a 2D/3D grinding model is developed to address the kinematics of each abrasive in infeed grinding process for $\phi 300\text{mm}$ silicon wafer. The cutting path and density is mathematically investigated and experimentally associated with the achievable surface roughness and the global flatness. The results are summarized as follows;

- 1) The cutting path pattern is only determined by the speed ratio n_2/n_1 of the wafer against the wheel, not the individual speed.
- 2) When $n_2/n_1 = 0.5$ the cutting path formed is a straight line. Other than that, lines are curved.
- 3) The cutting path density in the wafer center is higher than that at the fringe. The achieved surface roughness is inconsistent over the whole wafer.
- 4) The removal depth into the wafer is proportional to the cutting path density. The variation in the cutting path density leads the ground wafer to a concaved profile.
- 5) A proper tilt (alignment) between the wheel and wafer is able offset the effect of the cutting path density.

Acknowledgement

This research was partially sponsored by the Regional Consortium from New Energy and Industrial Technology Development Organization, the Grand-in-Aid for Exploratory Research (No.10875029) and the Regional Joint Research (No. 11792007) from the Ministry of Education, Science and Culture of Japan.

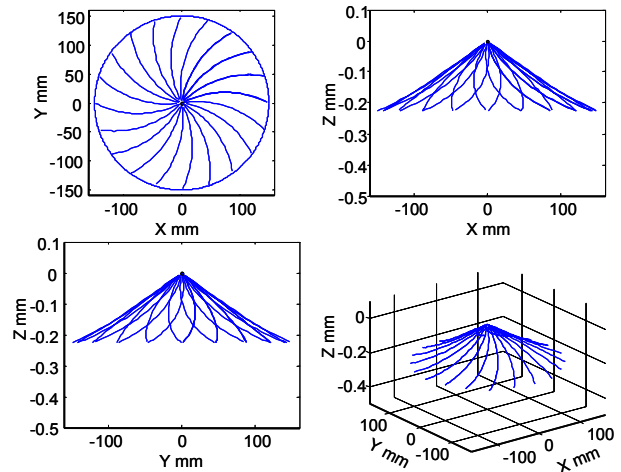


Fig. 8 $\alpha = \pm 0.1^\circ$

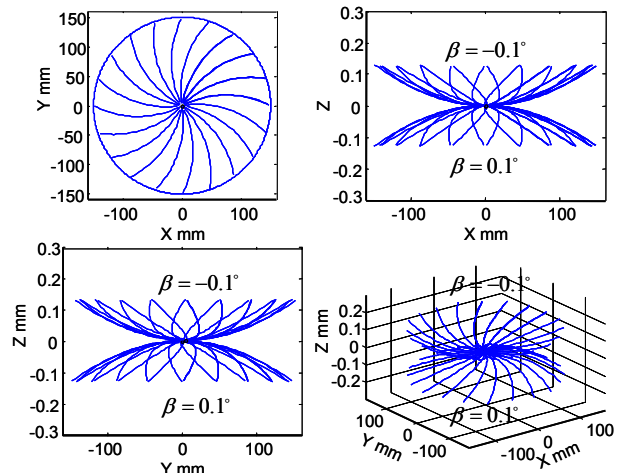


Fig. 9 $\beta = 0.1^\circ, \beta = -0.1^\circ$

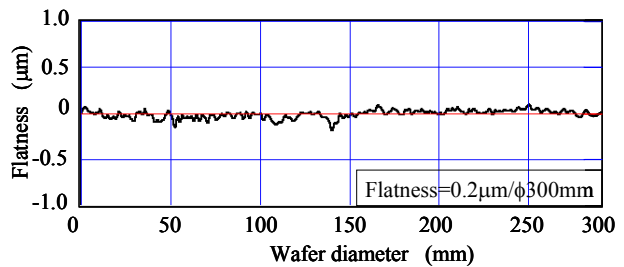


Fig. 10 Achieved flatness

References

- [1] L.ZHOU, H. EDA, et.al.: "Development of One-stop Machining System for $\phi 300\text{mm}$ Silicon Wafer, Proc. of ASPE 2000, 140-143.
- [2] K. Kimura, et.al.: Characteristics of CMP Using Hard Wheel Pad, Proc. of JSPE 1988, 245.
- [3] Töshoff H.K., Schmieden W.V., Inasaki I., König W. and Spur G., 1990, Abrasive Machining of Silicon, Annals of CIRP, 39/2, 621-635.